Aqueous Electrodeposition of Ge Monolayers

ARTICLE *in* LANGMUIR · NOVEMBER 2009

Impact Factor: 4.46 · DOI: 10.1021/la902929j · Source: PubMed

4 AUTHORS, INCLUDING:

Youn-Geun Kim
California Institute of Technology
86 PUBLICATIONS **790** CITATIONS

SEE PROFILE

John L. Stickney
University of Georgia
177 PUBLICATIONS **3,358** CITATIONS

SEE PROFILE

Langmuir Article

pubs.acs.org/Langmuir

Aqueous Electrodeposition of Ge Monolayers

Xuehai Liang, Youn-Geun Kim, Daniel K. Gebergziabiher, and John L. Stickney*

Department of Chemistry, The University of Georgia, Athens, Georgia 30602

Received August 7, 2009. Revised Manuscript Received October 1, 2009

The electrodeposition of germanium on Au(111) in aqueous solutions has been investigated by means of cyclic voltammetry, Auger electron spectroscopy, and in situ scanning tunneling microscopy (STM). The data yield a picture of germanium deposition, which starts with the formation of two well-ordered hydroxide phases, with $^1/_3$ ML and $^4/_9$ ML coverages upon initial reduction of the Ge(IV) species (probably H_2GeO_3 at pH 4.7). Those structures appear to result from a three-electron reduction to form surface-limited structures with $(\sqrt{3} \times \sqrt{3})R30°$ or (3×3) unit cells, respectively. Further reduction, probably in a two-electron process from the hydroxide structures, resulted in a germanium hydride structure, again surface-limited, with a coverage of close to 0.8 ML. The hydride structure is very flat, though with the periodic modulation characteristic of a Moiré pattern. Longer deposition times and lower potentials resulted in increased coverage of Ge in some cases, but with apparently limited coverage as a function of pH. The maximum Ge coverage, about 4 ML, was observed using a pH 9.32 deposition solution. At potentials negative of the Moiré pattern, about −850 mV versus Ag/AgCl, a "corruption" of the smooth Moiré pattern occurred. This roughening appears to mark the initial formation of a Au−Ge alloy, accounting for the observation of coverage in excess of that needed to form the Moiré pattern at some pH values.

Introduction

The group IV element germanium is and has been of great importance in electronics and materials science.[1−4] Compared with silicon, Ge has about twice the electron mobility and about four times the hole mobility, suggesting that in certain applications it should have higher performance than silicon (e.g., for channel devices).[5] In addition, Ge is known as an important material in optics, given its small band gap of 0.67 eV, which allows it to respond to infrared light efficiently.[6]

A simple methodology for the formation of Ge thin films would have important consequences for the viability of Ge in the formation of various device structures. Vapor deposition is a reasonable methodology and has been studied and improved by a number of workers.[3,7,8] Ge deposition via molecular beam epitaxy is well understood and high-quality films can be formed, but the technology is still prohibitive for some applications.[9]

Attempts have been made to form high-quality Ge films using electrodeposition as a way to improve structure control, achieve selective deposition, and devise a low-cost deposition methodology. Because of the reactivity of germanium ions in aqueous solution,[10,11] most investigators have used nonaqueous solvents or ionic liquids. Ge deposition on a variety of substrates in ionic liquids and nonaqueous solvents[12−16] has been studied by several groups (Endres, Saitou, Huang, etc.). Endres studied the electrodeposition process of Ge on Au substrates in the ionic liquid (1-butyl-3-methylimidazolium-hexafluorophosphate) using a unique home-built STM design.[17,18] High-quality images of the Ge deposits were obtained. The band gaps of the films made in the ionic liquid were investigated using I/U tunneling spectroscopy. A symmetrical band gap of 0.7 eV was found for films ⩾100 nm thick. Endres also deposited Ge nanowires and 3D-ordered macroporous Ge at bulk deposition potentials using templates.[19,20] Huang reported the deposition of bulk Ge thin films on Si substrates in 1,3-propanediol and how the Si substrates affected the deposition and crystallization.[16]

One promising technology involving Ge is the formation of phase-change materials, such as $Ge_xSb_yTe_z$ (GST).[21−25] GST is a very promising candidate for making the next generation of data

*Corresponding author. E-mail: stickney@chem.uga.edu.

(1) Patel, N.; Ramesha, A.; Mahapatra, S. *Microelectron. J.* **2008**, *39*, 1671–1677.
(2) Chong, T. C.; Shi, L. P.; Qiang, W.; Tan, P. K.; Miao, X. S.; Hu, X. *J. Appl. Phys.* **2002**, *91*, 3981–3987.
(3) King, T. J.; Saraswat, K. C. *J. Electrochem. Soc.* **1994**, *141*, 2235–2241.
(4) Solomon, A.; Fengnian, X.; Stephen, W. B.; Ying, Z.; Teya, T.; Philip, M. R.; Yurii, A. V. *CMOS-Integrated 40 GHz Germanium Waveguide Photodetector for On-Chip Optical Interconnects*; Optical Fiber Communication Conference, 2009; Optical Society of America, 2009; p OMR4.
(5) Shang, H.; Frank, M. M.; Gusev, E. P.; Chu, J. O.; Bedell, S. W.; Guarini, K. W.; Ieong, M. *IBM J. Res. Dev.* **2006**, *50*, 377–386.
(6) Ballato, J.; Hawkins, T.; Foy, P.; Yazgan-Kokuoz, B.; Stolen, R.; McMillen, C.; Hon, N. K.; Jalali, B.; Rice, R. *Opt. Express* **2009**, *17*, 8029–8035.
(7) Medeiros-Ribeiro, G.; Bratkovski, A. M.; Kamins, T. I.; Ohlberg, D. A. A.; Williams, R. S. *Science* **1998**, *279*, 353–355.
(8) Li, V. Z. Q.; Mirabedini, M. R.; Kuehn, R. T.; Wortman, J. J.; Ozturk, M. C.; Batchelor, D.; Christensen, K.; Maher, D. M. *Appl. Phys. Lett.* **1997**, *71*, 3388–3390.
(9) Lee, M. L.; Pitera, A. J.; Fitzgerald, E. A. *J. Vac. Sci. Technol., B* **2004**, *22*, 158–164.
(10) Jayakrishnan, S.; Pushpavanam, M.; Shenoi, B. A. *Surf. Technol.* **1981**, *13*, 225–240.
(11) Fink, C. G.; Dokras, V. M. *J. Electrochem. Soc.* **1949**, *95*, 80–97.
(12) Endres, F.; El Abedin, S. Z. *Chem. Commun.* **2002**, *8*, 892–893.
(13) Endres, F. *Phys. Chem. Chem. Phys.* **2001**, *3*, 3165–3174.
(14) Al-Salman, R.; Abedin, S. Z.; Endres, F. *Phys. Chem. Chem. Phys.* **2008**, *10*, 4650–4657.
(15) Saitou, M.; Sakae, K.; Oshikawa, W. *Surf. Coat. Technol.* **2003**, *162*, 101–105.
(16) Huang, Q.; Bedell, S. W.; Saenger, K. L.; Copel, M.; Deligianni, H.; Romankiw, L. T. *Electrochem. Solid State Lett.* **2007**, *10*, D124–D126.
(17) Endres, F.; El Abedin, S. Z. *Phys. Chem. Chem. Phys.* **2002**, *4*, 1649–1657.
(18) Endres, F.; El Abedin, S. Z. *Phys. Chem. Chem. Phys.* **2002**, *4*, 1640–1648.
(19) Al-Salman, R.; Mallet, J.; Molinari, M.; Fricoteaux, P.; Martineau, F.; Troyon, M.; El Abedin, S. Z.; Endres, F. *Phys. Chem. Chem. Phys.* **2008**, *10*, 6233–6237.
(20) Meng, X. D.; Al-Salman, R.; Zhao, J. P.; Borissenko, N.; Li, Y.; Endres, F. *Angew. Chem., Int. Ed.* **2009**, *48*, 2703–2707.
(21) Nonaka, T.; Ohbayashi, G.; Toriumi, Y.; Mori, Y.; Hashimoto, H. *Thin Solid Films* **2000**, *370*, 258–261.
(22) Zhang, Y.; Wong, H. S. P.; Raoux, S.; Cha, J. N.; Rettner, C. T.; Krupp, L. E.; Topuria, T.; Milliron, D. J.; Rice, P. M.; Jordan-Sweet, J. L. *Appl. Phys. Lett.* **2007**, *91*, 3.
(23) Morales-Sánchez, E.; Prokhorov, E. F.; González-Hernández, J.; Mendoza-Galván, A. *Thin Solid Films* **2005**, *471*, 243–247.
(24) Lee, J.; Choi, S.; Lee, C.; Kang, Y.; Kim, D. *Appl. Surf. Sci.* **2007**, *253*, 3969–3976.
(25) Kim, R. Y.; Kim, H. G.; Yoon, S. G. *Appl. Phys. Lett.* **2006**, *89*, 3.

storage materials. It is capable of high storage capacity, data rate reading, writing, and erasing as well as high cyclability and long archival life. Until recently, this material has been formed using only vapor deposition methods.

The work in this group has focused on the development of an electrochemical version of atomic layer deposition (ALD).[26−30] ALD is based on the use of surface-limited reactions to form deposits one atomic layer at a time: layer-by-layer growth. In principle, this minimizes surface roughening with growth and allows control over deposit thickness with atomic-layer accuracy. The method appears to have important applications in the area of electronic materials, given the need for conformal nanofilm formation.

Surface-limited reactions in electrodeposition are generally referred to as underpotential deposition (UPD).[17,31−33] UPD is a phenomenon where an element can be deposited on a second element, forming a single atomic layer, by use of a potential prior to (under) that needed to form a bulk deposit of the element. UPD results from the free energy of surface compound or alloy formation, where the first atomic layer of an element is stabilized by bonding to the second element. The UPDs of both Te and Sb on Au in aqueous solution have been the subject of studies by our group and others.[34−38] However, little work has been done toward an atomic-level understanding of Ge electrodeposition in aqueous solution. Recently, the alternated deposition of Sb and Te has been reported with respect to the formation of phase-change materials by a group at IBM, Watson.[30,39] In the IBM work, single-crystalline Sb_2Te_3 films were deposited onto Au and TiN by EC-ALD in aqueous solution.

The impetus for the present studies was the need to understand the first stages of Ge electrodeposition better, especially the first atomic layer and subatomic layer, and the possibility of forming Ge atomic layers in aqueous solution. The idea was that if a method for the formation of Ge atomic layers could be developed and combined with Te and Sb UPD then a cycle for the growth of GST might be developed in aqueous solution, as might a program for other Ge-containing compounds.

Experimental Section

The hardware used to form deposits has been described previously[40] (Electrochemical ALD L.C., Athens, GA). The system consisted of pumps, valves, an electrochemical flow cell, and a potentiostat, all computer-controlled with specialized software. Solutions, valves, and tubing were confined inside a nitrogen-purged Plexiglas box to exclude oxygen. The flow cell was similar to that described in ref 40, though the auxiliary electrode has been changed from ITO to a Au wire imbedded in the cell wall opposite the deposit area for a simple primary current distribution. The reference electrode was Ag/AgCl (3 M NaCl) (Bioanalytical Systems, Inc., West Lafayette, IN). Substrates consisted of 300-nm-thick gold films formed on 10 nm Ti adhesion layers on glass slides. The deposits were annealed at 400 °C for 12 h, under a vacuum of 10^{-6} Torr after deposition, and resulted in a [111] habit. During deposition, a low flow rate was used (10 mL/min), and the solutions were kept flowing during the experiments in order to promote the steady state and prevent the buildup of byproduct in the cell from the auxiliary electrode. A majority of the electrochemical experiments were performed by starting at 500 mV, scanning to a potential, and holding for a set period of time. Characterization of the voltammetry and its comparison with other experiments led to increased confidence that the conditions were reproducible. A statement such as "the potential was held at −800 mV" means that the clean electrode was started at 500 mV and scanned to −800 mV, where it was held for the stated period of time. Cyclic voltammetry of a gold substrate in 0.1 M H_2SO_4 was used to check substrate cleanliness.

In-situ scanning tunneling microscopy studies were performed using a Nanoscope III (Digitial Instruments, Veeco), equipped with W tips that were electrochemically etched (15 V ac in 1 M KOH) from 0.25 mm wires. The tip was coated with transparent nail polish to minimize faradaic currents from the tip sides.[33,41] The electrodes used were gold single-crystal beads made in-house using a variation of the Clavilier method.[42,43] Imaging was performed on one of the resulting large Au(111) planes. Experiments were begun with a clean Au(111) surface in a H_2GeO_3 solution (depending on the pH) at a potential positive of H_2GeO_3 reduction. STM images were taken in situ at a number of potentials as the potential was shifted negatively from 500 mV. The potential was held for approximately 3 min while images were collected.

For UHV-EC studies, a disk-shaped Au(111) single-crystal substrate was used. The Au(111) substrate was cleaned by ion bombardment with 200 eV argon ions and then annealed to produce the characteristic hexagonal LEED pattern.[44,45] Electrochemical reactions were performed in a stainless steel antechamber on the UHV surface analysis instrument, which contained an electrochemical cell. The antechamber was backfilled with UHP Ar during electrochemical experiments. After reaction, the electrochemical cell was drained and removed through a gate valve so that the antechamber could be pumped to UHV. That procedure prevented exposure of the samples to the atmosphere and facilitated the direct transfer back into the UHV analysis chamber. The surface composition was then characterized using Auger electron spectroscopy.[33,45,46]

A series of Ge(IV) solutions differing in pH (pH 1.21, 4.72, 9.32, 12.36, and 12.93) and concentration (0.5, 1, and 10 mM) were investigated. All solutions used contained 0.5 M sodium sulfate as a supporting electrolyte, except for the Auger experiments where a more dilute (0.01 M sodium sulfate) solution was used. Water used for solutions was supplied from a Nanopure water filtration system (Barnstead, Dubuque, IA) attached to the house DI water system. Chemicals were reagent grade or better. All solutions were purged with nitrogen before and during experiments in order to minimize the oxygen concentration.

(26) Banga, D. O.; Vaidyanathan, R.; Liang, X. H.; Stickney, J. L.; Cox, S.; Happeck, U. *Formation of PbTe Nanofilms by Electrochemical Atomic Layer Deposition (ALD)*; Pergamon-Elsevier Science Ltd: 2008; pp 6988−6994.
(27) Thambidurai, C.; Kim, Y. G.; Stickney, J. L. *Electrochim. Acta* **2008**, *53*, 6157–6164.
(28) Muthuvel, M.; Stickney, J. L. *Langmuir* **2006**, *22*, 5504–5508.
(29) Venkatasamy, V.; Jayaraju, N.; Cox, S. M.; Thambidurai, C.; Stickney, J. L. *J. Electrochem. Soc.* **2007**, *154*, H720–H725.
(30) Venkatasamy, V.; Shao, I.; Huang, Q.; Stickney, J. L. *J. Electrochem. Soc.* **2008**, *155*, D693–D698.
(31) Vaidyanathan, R.; Cox, S. M.; Happek, U.; Banga, D.; Mathe, M. K.; Stickney, J. L. *Langmuir* **2006**, *22*, 10590–10595.
(32) Villegas, I.; Napolitano, P. *J. Electrochem. Soc.* **1999**, *146*, 117–124.
(33) Kim, Y. G.; Kim, J. Y.; Thambidurai, C.; Stickney, J. L. *Langmuir* **2007**, *23*, 2539–2545.
(34) Ward, L. C.; Stickney, J. L. *Phys. Chem. Chem. Phys.* **2001**, *3*, 3364–3370.
(35) Lay, M. D.; Stickney, J. L. *J. Electrochem. Soc.* **2004**, *151*, C431–C435.
(36) Sorenson, T. A.; Varazo, K.; Suggs, D. W.; Stickney, J. L. *Surf. Sci.* **2001**, *470*, 197–214.
(37) Sorenson, T. A.; Suggs, D. W.; Nandhakumar, I.; Stickney, J. L. *J. Electroanal. Chem.* **1999**, *467*, 270–281.
(38) Wu, Q.; Shang, W. H.; Yan, J. W.; Mao, B. W. *J. Mol. Catal A: Chem.* **2003**, *199*, 49–56.
(39) Huang, Q.; Kellock, A. J.; Raoux, S. *J. Electrochem. Soc.* **2008**, *155*, D104–D109.
(40) Flowers, B. H.; Wade, T. L.; Garvey, J. W.; Lay, M.; Happek, U.; Stickney, J. L. *J. Electroanal. Chem.* **2002**, *524−525*, 273–285.
(41) Lay, M. D.; Sorenson, T. A.; Stickney, J. L. *J. Phys. Chem. B* **2003**, *107*, 10598–10602.
(42) Clavilier, J.; Armand, D.; Sun, S. G.; Petit, M. *J. Electroanal. Chem.* **1986**, *205*, 267–277.
(43) Feliu, J. M.; Rodes, A.; Orts, J. M.; Clavilier, J. *Pol. J. Chem.* **1994**, *68*, 1575–1595.
(44) Lister, T. E.; Stickney, J. L. *J. Phys. Chem.* **1996**, *100*, 19568–19576.
(45) Kim, J. Y.; Kim, Y. G.; Stickney, J. L. *J. Electrochem. Soc.* **2007**, *154*, D260–D266.
(46) Kim, Y. G.; Kim, J. Y.; Vairavapandian, D.; Stickney, J. L. *J. Phys. Chem. B* **2006**, *110*, 17998–18006.

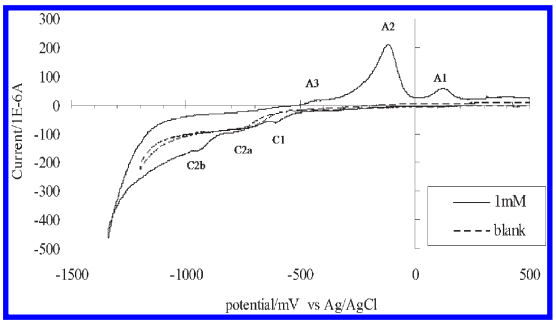

Figure 1. Cyclic voltammetry of gold in a 0.5 M Na_2SO_4 pH 4.72 blank solution (---) and a 0.5 M Na_2SO_4 + 1 mM GeO_2 pH 4.72 solution (−). Electrode area, 3 cm^2; scan rate, 5 mV/s.

Results

GeO_2 Solution, 1 mM, pH 4.7, No Buffer. Figure 1 shows the cyclic voltammetry results for a gold substrate in a pH 4.72 GeO_2 solution. From the Pourbaix diagram[47] at pH 4.7, GeO_2 should exist mostly in the form of H_2GeO_3. The scan in Figure 1 started at 500 mV, positive of any reduction process for H_2GeO_3, and was scanned negatively at 5 mV/s. Three reduction features (C1, C2a, and C2b) are evident, before extensive hydrogen evolution, at −1300 mV. Upon reversal of the scan direction, three oxidation features were evident—peaks A3, A2, and A1. Peaks A1 and C1 as well as A2 and C2a,b appear to correspond to the inverses of their specific reactions. One feature (C3) is not evident in this CV but will be noted later; it is the inverse of A3.

To understand the deposition process better, in-situ STM and Auger spectroscopy were used to characterize the deposit structure and composition, respectively. From Figure 1, it appears that deposition began around −350 mV. The in-situ STM images shown in Figure 2 were obtained at −500 mV. Domains of both $(\sqrt{3} \times \sqrt{3})R30°$ and (3×3) structures are evident. The darker areas are domains of a $^1/_3$ ML coverage $(\sqrt{3} \times \sqrt{3})R30°$ structure, and the lighter (higher) are domains of a $^4/_9$ ML (3×3) structure. In this report, the definition of a monolayer (ML) is based on the number of substrate surface atoms: 1 ML corresponds to one surface species for every surface atom. The domains in Figure 2 differ in height by less than 0.1 nm, as evident in the line scan in Figure 2. The larger height differences in the line scan are due to atomic steps in the Au substrate. At more negative potentials, domains of the $(\sqrt{3} \times \sqrt{3})R30°$ structure converted to the (3×3), as a few more Ge species deposit, shifting the coverage from $^1/_3$ ML to $^4/_9$ ML. Holding the potential at −600 mV (peak C1, Figure 1) resulted in the eventual conversion of all domains to the $^4/_9$ ML (3×3) structure (Figure 3). A subsequent positive scan from −600 mV showed increases in peak A1 until the $^4/_9$ ML (3×3) was complete, at which point the charge for peak A1 was limited. Figure 4 displays four CV curves, where the potential was held at −600 mV for different periods of time. There are two peaks evident, A3 and A1. A3 will be discussed subsequently, but it is clear that after about 500 s peak A1 is limited to a charge of about 0.77 mC (peak A1, Figure 4). If the surface of the Au on glass films is assumed to be best represented as a Au(111) surface with an atomic density of 1.4×10^{15} atoms/cm^2, then 2.2×10^{-4} C/cm^2 would be required for 1 ML of a one-electron process, neglecting surface roughness. The working electrode surface area used was 3 cm^2, so a coverage of $^4/_9$ ML (0.44 ML) would require 2.9×10^{-4} C/electron. Because the charge measured for A1 was 7.7×10^{-4} C (i.e., roughly 3 times as much as for other peaks),

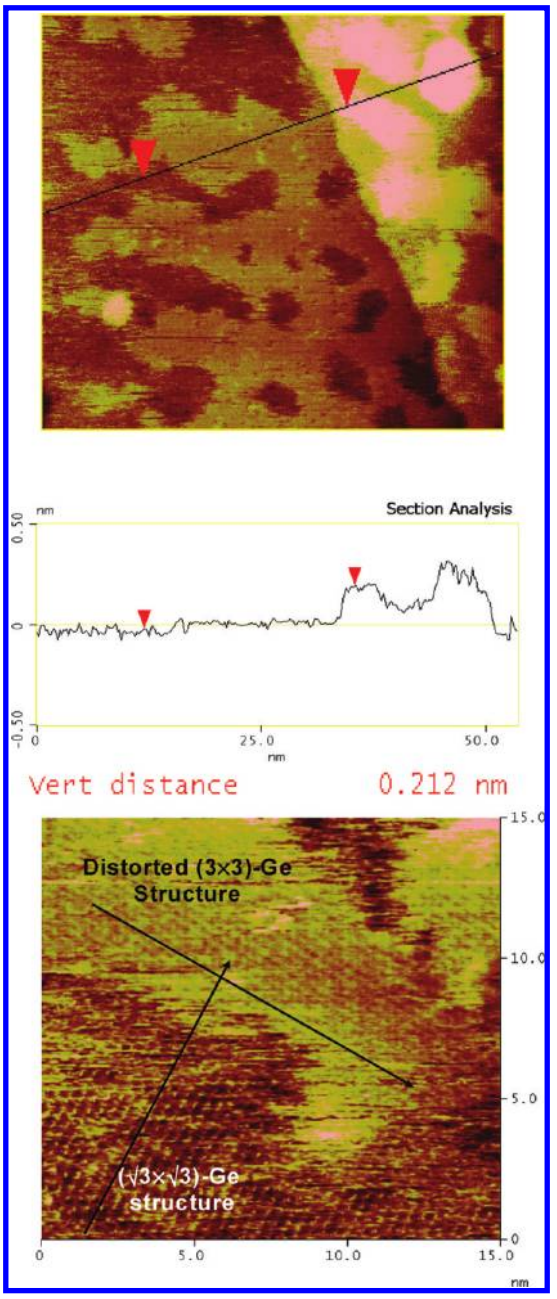

Figure 2. STM images of Ge deposited on Au(111) at −500 mV in a 0.5 M Na_2SO_4 + 1 mM GeO_2 pH 4.72 solution.

a three-electron process is assumed. This would indicate that A1 corresponds to the oxidation of an adsorbed Ge species in the +1 oxidation state, $GeOH_{(ad)}$ for instance, to soluble H_2GeO_3 (a Ge(IV) species), as described by eq 1.

That the charge for the oxidation of this hydroxide layer is maximized suggests that it is a surface-limited reaction or an underpotential deposition (UPD) process. The majority of UPD processes result in an atomic layer of the element in the zero oxidation state. In this case, however, UPD appears to involve the formation of a hydroxide structure.

Peak A3 in Figure 4 grew with time in a fashion similar to that for A1. To understand peak A3 better, the experiment shown in Figure 5 was performed. The potential of the clean Au substrate was scanned from 500 mV in the H_2GeO_3 solution to −600 mV (the dotted line), where it was held for 500 s. Under these conditions, the coverage should be $^4/_9$ ML, as it is for the (3×3)

(47) Pourbaix, M. *Atlas of Electrochemical Equilibira in Aqueous Solution*; Pergamon Press: New York, 1966.

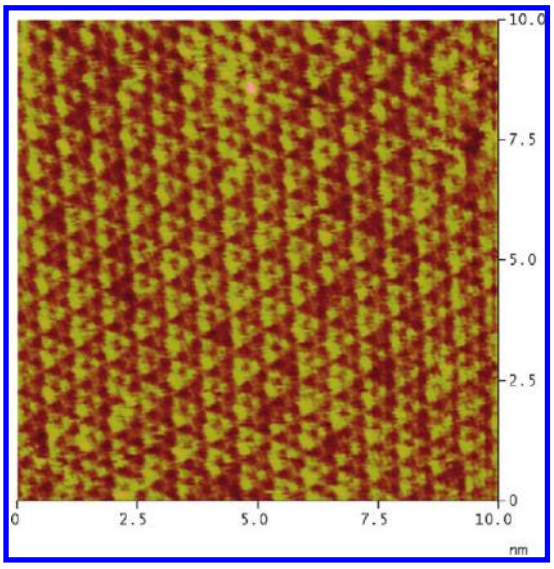

Figure 3. STM image of Ge deposited on Au(111) at −600 mV in a 0.5 M Na_2SO_4 + 1 mM GeO_2 pH 4.72 solution.

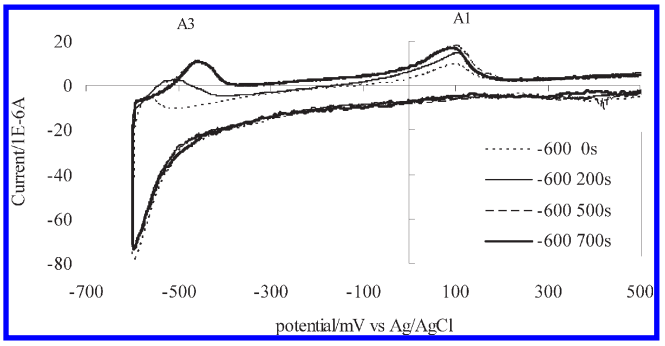

Figure 4. Cyclic voltammetry of holding gold in a 0.5 M Na_2SO_4 + 1 mM GeO_2 pH 4.72 solution at −600 mV for different times. Electrode area, 3 cm^2; scan rate, 5 mV/s.

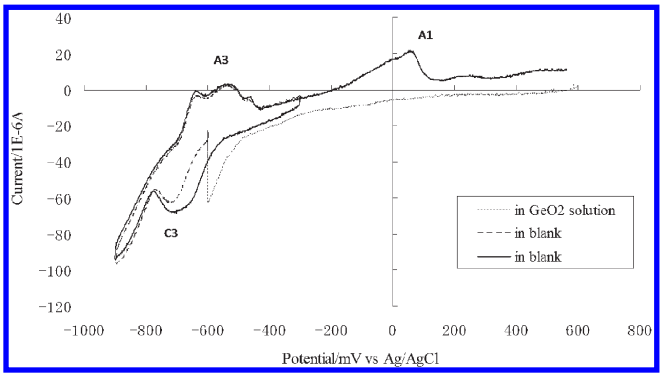

Figure 5. Cyclic voltammetry of (3 × 3)-structured Ge (UPD) in a 0.5 M Na_2SO_4 pH 4.72 blank solution.

structure shown in Figure 3. These deposits were run using a flow cell, as previously described,[40] so it was a simple matter to exchange the H_2GeO_3 solution for the corresponding blank to prevent the subsequent reaction of H_2GeO_3 solution species as the potential was scanned to more negative potentials. Thus, the total coverage of Ge species on the surface was held at $^4/_9$ ML and did not change as the scan was continued (dashed line) to −900 mV, resulting in a prominent reduction peak, C3, at −700 mV prior to extensive hydrogen evolution (below −800 mV). Note that in Figure 1 there was no C3 noted because the C2 process was convoluted with C3. By exchanging the H_2GeO_3 solution for the blank, C3 is clearly evident where the C2 process has been eliminated. Peak A3 (Figure 5) is evident as well, though it appears to be broken into three subpeaks. Once positive of the A3 peaks, the scan was reversed at −300 mV and scanned back to −900 mV (solid line), so the total charge under peak C3 could be determined without the influence of holding the potential at −600 mV (dashed scan in Figure 5) or any reaction from solution-phase H_2GeO_3. That both the solid and dashed lines for A3 have the same morphology suggests that there was no significant coverage difference between the two. By estimating baselines for C3 and A3, assuming a background of hydrogen evolution and some oxygen reduction, the integration of peaks C3 and A3 resulted in -4.7×10^{-4} and 4.8×10^{-4} C for peaks C3 and A3, respectively. The ratio of the A3 charge (4.8×10^{-4}) to the A1 charge, 7.4×10^{-4} C (Figure 5), is 2/3. Thus, if peak A1 is a three-electron oxidation of a (3 × 3) $GeOH_{(ad)}$ structure to soluble Ge(IV) species (eq 1), then a 2/3 ratio suggests that peak A3 is Ge in a −1 oxidation state (a hydride) converting to $GeOH_{(ad)}$ in a two-electron oxidation (eq 2). In-situ infrared spectroscopy studies of the Ge surface under similar conditions[48−51] suggested that stable Ge surface species in an aqueous solution are either hydride or a hydroxide species. There was little evidence in those studies of a Ge° species at any potential.

On the basis of the coulometry in Figure 5, at −800 mV, where hydrogen evolution becomes extensive, the deposited Ge species on the surface should be predominately GeH.[48] At still more negative potentials, some GeH_2 species or other kinds of germanium hydrides may have formed, accounting for the split A3 peak.[16,52,53] A suggested deposition mechanism is

$$H_2GeO_3 + 3e^- + 3H^+ = GeOH_{(ad)} + 2H_2O \quad (1)$$

$$GeOH_{(ad)} + 2e^- + 2H^+ = GeH_{(ad)} + H_2O \quad (2)$$

$$GeH_{(ad)} + e^- + H^+ = GeH_{2(ad)} \quad (3)$$

The graph shown in Figure 6a displays the Auger signals for O and Ge as a function of potential. The data in Figure 6 was obtained by the immersion of a clean Au(111) single crystal into a pH 4.5 solution of 2 mM K_2SO_4 containing 0.1 mM H_2GeO_3 at open circuit and then scanning to the potential listed and holding for 2 min. Au(111) was then immersed (withdrawn) from the solution and (after pumping down) transferred back to the UHV analysis chamber. As can be seen, the solution used was not exactly the same as those used for Figures 4 and 5 but was purposely diluted to minimize any electrolyte immersed with the sample. Samples immersed in more concentrated solutions frequently became coated with salt crystals upon evacuation and transfer to the analysis chamber.[33] In addition, potassium sulfate was used instead of sodium sulfate because potassium shows up better in Auger, allowing counterions to be monitored. Problems

(48) Maroun, F.; Ozanam, F.; Chazalviel, J. N. *Surf. Sci.* **1999**, *428*, 184–189.
(49) Maroun, F.; Chazalviel, J. N.; Ozanam, F.; Lincot, D. *J. Electroanal. Chem.* **2003**, *549*, 161–163.
(50) Ehlers, C.; Konig, U.; Staikov, G.; Schultze, J. W. *Electrochim. Acta* **2001**, *47*, 379–385.
(51) Maroun, F.; Ozanam, F.; Chazalviel, J. N. *Chem. Phys. Lett.* **1998**, *292*, 493–499.
(52) Maroun, F.; Ozanam, F.; Chazalviel, J. N. *J. Phys. Chem. B* **1999**, *103*, 5280–5288.
(53) Chazalviel, J. N.; Belaidi, A.; Safi, M.; Maroun, F.; Erne, B. H.; Ozanam, F. *Electrochim. Acta* **2000**, *45*, 3205–3211.

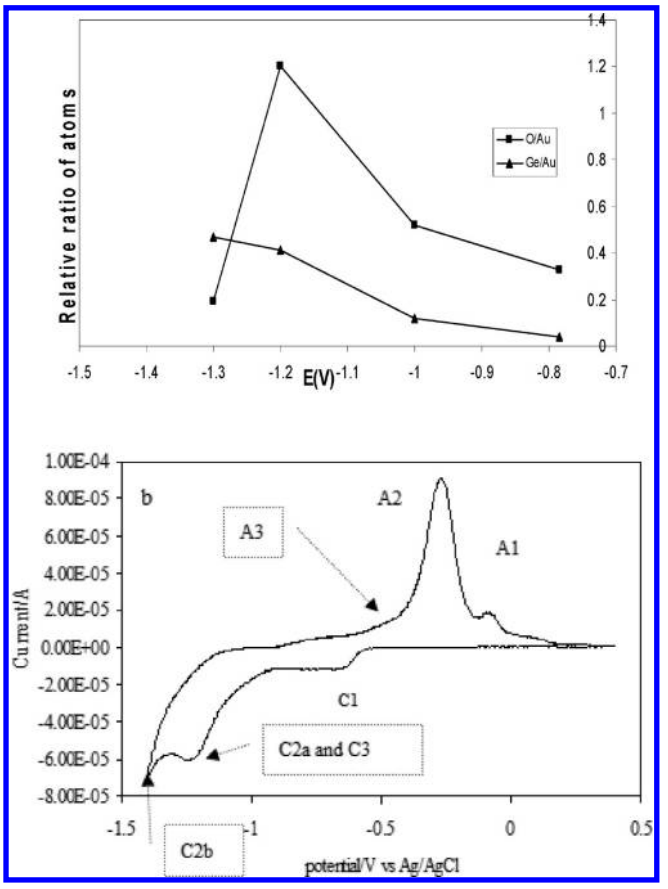

Figure 6. (a) Auger peak-to-peak ratio of atoms at different potentials. (b) Cyclic voltammetry of Au(111) in 0.1 mM GeO_2 and 2 mM K_2SO_4 at pH 4.5. Scan rate, 5 mV/s.

associated with using this more dilute solution, and no buffer, were peak potential shifts. At higher currents, peaks shifted because of an IR drop, given the increase in solution resistance for the dilute solutions. In addition, these reactions are very sensitive to pH, and the lack of a buffer, together with some hydrogen evolution, may further account for observed potential shifts. As a result, in Figure 6b, peak C3 (which overlaps with peak C2a) begins to appear just below −1200 mV instead of at −700 mV, as in Figure 5. From the graph in Figure 6a, the oxygen maximum occurred at −1200 mV and then dropped dramatically at more negative potentials, consistent with peak C3 corresponding to hydroxide surface conversion to the hydride. Note the plateau in the Ge signal at negative potentials, consistent with a surface-limited reaction during the reduction of the hydroxide. That is, the Ge coverage did not change significantly as the oxygen coverage dropped by a factor of 6.

By comparing Figure 1 with Figure 5, where the H_2GeO_3 solution was removed from the cell, it is clear that C3 and C2 (C2a and C2b) overlap so that C3 does not appear as a defined peak in Figure 1. This region of the CV in the H_2GeO_3 solution thus corresponds to both the conversion of the (3×3) hydroxide structure to a hydride (C3) and to another process (C2)—the deposition of more Ge species. The net result is the formation of a hydride structure. How C2 results in more Ge species on the surface, the mechanism, is not clear; the C2 process may involve an adsorbed hydroxide intermediate or may be converted directly to an adsorbed hydride species.

At −800 mV, a Moiré pattern was observed with STM (Figure 7), corresponding to a coverage of 0.8 ML. Figure 8 shows the voltammetry after holding at −800 mV for 200 and

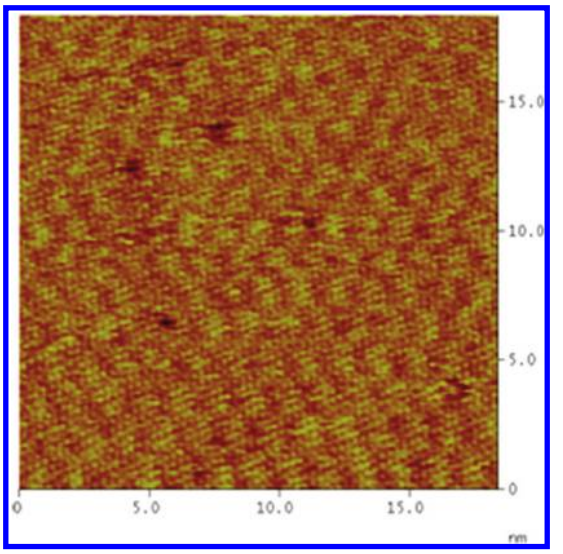

Figure 7. STM image of Ge deposited on Au(111) at −800 mV in a 0.5 M Na_2SO_4 + 1 mM GeO_2 pH 4.72 solution.

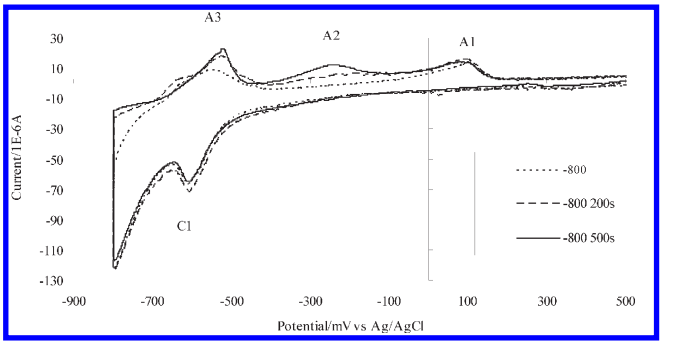

Figure 8. Cyclic voltammetry of holding gold in a 0.5 M Na_2SO_4 + 1 mM GeO_2 pH 4.32 solution at −800 mV for different time. Electrode area, 3 cm^2; scan rate, 5 mV/s.

500 s, followed by scanning positively. There was a significant increase in peaks A3 and A2 after holding for 200 s and a much smaller increase after waiting for 500 s. The charge under peaks A2 and A1 combined corresponded to 1.1×10^{-3} C, or a coverage of 0.62 ML for a three-electron process (oxidation of a layer of $GeOH_{(ad)}$ to H_2GeO_3) such as that described by eq 1. This can be compared to the 0.8 ML expected for the Moiré pattern, which suggests that the accumulation of sufficient GeH to form the Moiré pattern was a slow process at −800 mV, and in Figure 8, some domains of the $^4/_9$ ML coverage (3×3) hydroxide were still present. For deposits formed using potentials negative of −800 mV (Figure 8), the coverage of Ge species increased further. The difficulty in completing the Moiré structure (Figure 7) probably stemmed from slow kinetics, resulting in the need for an overpotential to drive the process. This is similar to the issues experienced in the formation of atomic layers of chalcogenides, where an overpotential was required to form surface-limited deposits, but because of their slow kinetics, some bulk was inevitably deposited as well.[30]

The surface formed at −800 mV, covered with the Moiré structure, was atomically flat over large (300 nm) domains (Figure 9a). However, shifting the potential to −880 mV produces images that show a dramatic increase in roughness (Figures 9b,c). Stepping the potential back to −750 mV appeared to repair the roughness, renewing the large flat planes characteristic of the Moiré structure (Figure 9d,e). The nature of that roughening

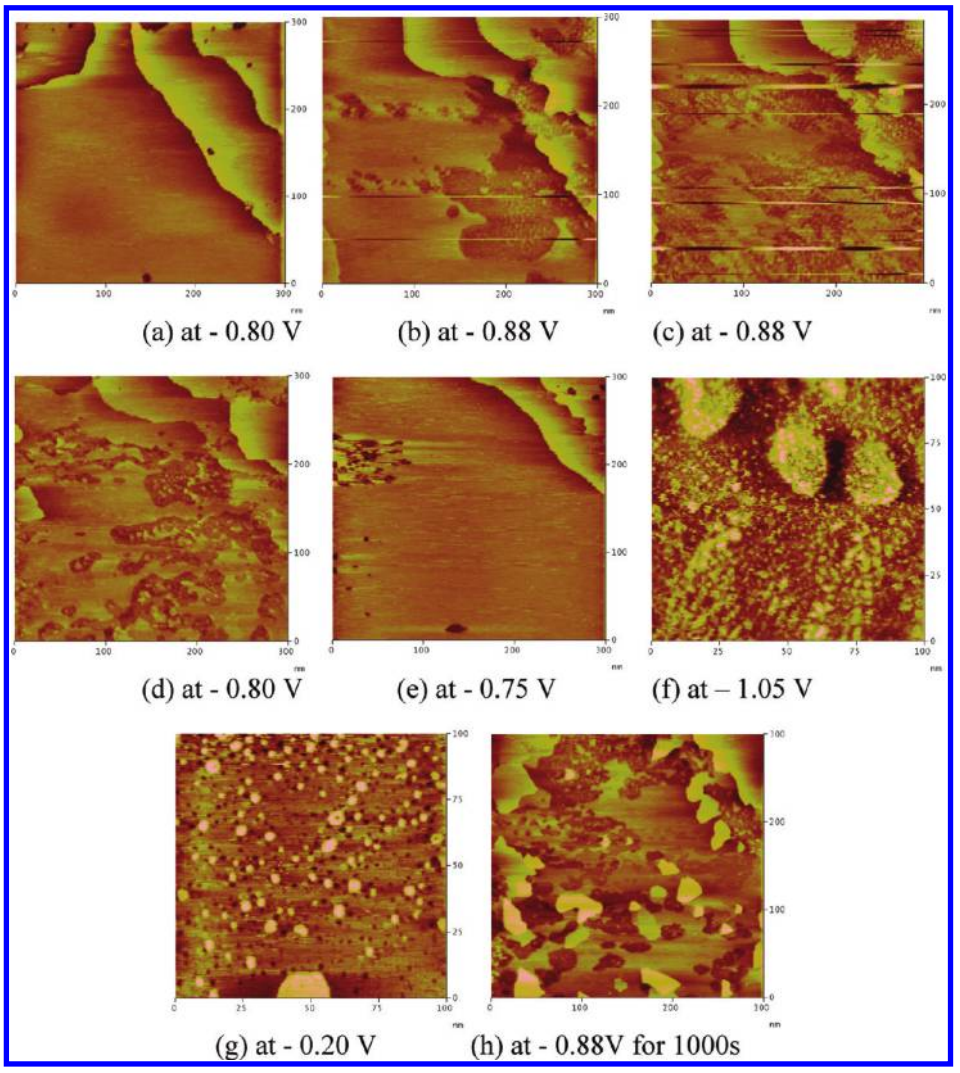

Figure 9. STM images of the deposited Ge surface changing with potentials in a 0.5 M Na_2SO_4 + 1 mM GeO_2 pH 4.72 solution.

transition is not clear from the data collected in this study. Initially, it was assumed that some of the $GeH_{(ad)}$ species were reduced further to a soluble Ge species such as GeH_4, noted as a possible species in the Pourbaix diagram.[47] To investigate the possibility that the roughing was the result of dissolution, a series of experiments were performed where the charge for Ge stripping was compared for surfaces with the Moiré pattern structure. The charge for oxidative stripping remained the same, whether the deposit was held in blank solution at a potential of −800 mV, where the Moiré pattern was formed, or was shifted to −900 mV, where the roughening took place. If the roughening had involved the loss of Ge species, then the subsequent oxidative stripping charge should have decreased. It did not, suggesting that the roughening did not involve dissolution. In addition, from STM studies, the height differences between the flat Moiré domains and the areas where the Ge dissolution appeared to have taken place were measured to be about 0.1 nm. If a molecular species such as GeH were removed, then it is expected that considerably more then a 0.1 nm step would result. That suggests that the pits are not due to the loss of a Ge species and exposure of the Au substrate, for at least a 0.2 nm step would be expected.

If the pits evident in Figure 9 are not due to the loss of Ge, then a change in tunneling resistance or structure or both would be needed to account for the pits. In a separate STM study, the potential was first stepped to −1050 mV, where the whole surface (Figure 9f) looked like the pits in Figure 9b−d. The potential was then stepped back to −200 mV, where the $(\sqrt{3} \times \sqrt{3})R30°$ structure should have been present (Figure 9g). The resulting surface was generally flat but with small pits and some islands. This image is reminiscent of the dissolution of a surface alloy, where one element of the alloy has been stripped. Ge−Au surface alloys have been reported in two previous studies by Endres et al. and Wang et al.[17,54] Au is known as a mobile metal even at room temperature, so upon dissolution of the Ge alloy component, the resulting vacancies begin to coalesce into pits whereas Au adatoms Ostwald ripen, forming islands (Figure 9g). This suggests that the initiation of alloy formation between Au and Ge initiates the pit formation in Figure 9b−e. Martinyuk[55] mentioned that hydrogen atom recombination may help in the mixing of Ge and Au, and the initiation of hydrogen evolution is consistent with the potentials where the roughening starts.

Holding the potential at −880 mV for longer times or at more negative potentials increased the atomic-scale roughening of the Ge surface (Figure 9h). That image shows the presence of atomically flat islands on the surface, which appear to extend from step edges. That is, alloy formation appears to form around them to leave only small areas of the flat Moiré structure. At that point,

(54) Wang, J.; Li, M.; Altman, E. I. *Surf. Sci.* **2005**, *596*, 126–143.
(55) Matyushin, V. M.; Martinyuk, R. V. *Vacuum* **2002**, *68*, 269–273.

the ability to form the smooth Moiré structure by shifting the potential in the positive direction to −750 mV was lost. Evidently, the complexity of the surface roughening became too great to be reversed simply by using a more positive potential to reform the smooth surface.

The chemical nature of these surfaces is not clear. That the Moiré pattern structure was a layer of a $GeH_{(ad)}$ species is reasonable. The pits in the surface that appear at −880 mV seem to be from the formation of a GeAu alloy, but there is little evidence to go on. At negative potentials of ⩽−880 mV, besides alloy formation, more Ge species appear to deposit, as evidenced by the increase in stripping peak A2. Deposition of only the first low-coverage Ge hydroxide structures resulted in surface-limited stripping peaks (A3 and A1). However, as the coverage increased, by using longer times or more negative potentials, peak A2 increased. One explanation of peak A2 is that it accounts for the stripping of Ge from the bulk and any extra Ge species required to convert (3 × 3) to the Moiré pattern structure. A3 would be the oxidation of the top Ge layer from hydride to hydroxide. A1 would then be the stripping of the last layer of Ge species in contact with bulk Au, the (3 × 3) hydroxide structure, which might be thought of as an underpotential deposit.

Effect of pH on Ge Deposition. Figure 10 displays a series of scans for gold substrates in solutions of GeO_2 as a function of pH. (An acetate buffer was used for pH 4.72 and a borate buffer was used for pH 9.32.) pH clearly had a significant influence on Ge deposition, not only on the potentials and voltammetric morphology in the scans but also on the amounts of Ge deposited.

In Figure 10, pH 9.32 displays the highest Ge coverage. A series of studies were performed to investigate the total charge for the oxidation of deposited Ge species as a function of the potential and time used for deposition. Figure 11 shows the data for the pH 9.32 solution. From Figure 10, −900 mV corresponds to the beginning of C1, or the formation of the first atomic layer of a $GeOH_{(ad)}$ species. The Moiré structure was formed between −970 and −1000 mV (Figure 11). For those three potentials, the stripping charge clearly limited out after 200 s, as expected for surface-limited reactions. Deposition at more negative potentials (−1040 to −1350 mV) displayed an increase in charge at longer times, consistent with the slow formation of an alloy. At the lowest potentials, −1.3 and −1.35 V, the same oxidation charges were obtained after only 200 s, corresponding to the maximum amount of Ge deposited from the pH 9.32 solution. Previous workers[11] noted limited amounts of deposition as well from aqueous solutions and that the addition of chloride, sulfide, or phosphate did not have a noticeable effect on the resulting deposit coverage. In studies performed by this group, changes in the concentration of GeO_2 species had the expected effect of increasing the deposition rate but not affecting the resulting maximum amounts deposited for a given pH.

The charges for stripping peak A1 were essentially the same, regardless of the pH. STM images of deposits formed in the pH 1.21 and 9.32 solutions displayed the (3 × 3) structure evident in the pH 4.72 solution, suggesting that the same $^4/_9$ ML coverage (3 × 3) structure may have been formed at each pH. The Moiré pattern was also observed with in-situ STM in the pH 1.21 and 4.72 solutions. The existence of UPD and the Moiré pattern of Ge on Au in an ionic liquid has also been suggested by Endres.[17]

Scans in the more basic solutions were similar to those shown for pH 4.72 in Figure 8. The deposited amounts were limited but exceeded the $^4/_9$ ML expected for the (3 × 3) structure and were sufficient to form the 0.8 ML Moiré pattern for all pH values. Figure 12 shows the maximum charges (coverages) for the

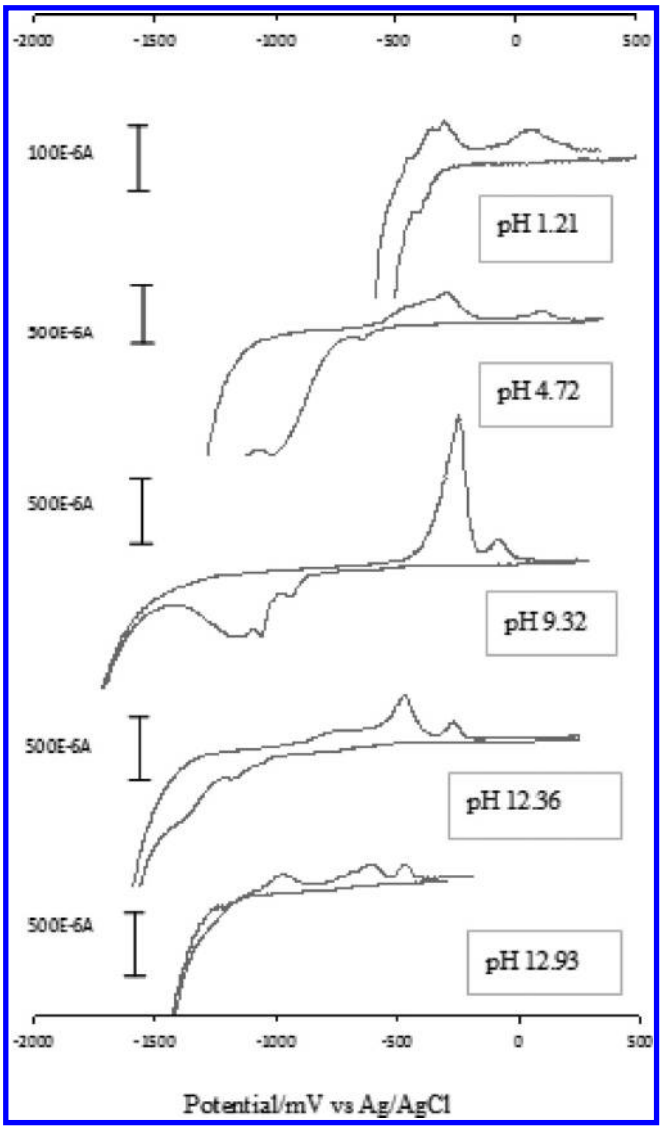

Figure 10. CVs of gold in 1 mM GeO_2 + 0.5 M Na_2SO_4 solutions of pH 1.21, 4.72, 9.32, 12.36, and 12.93. Electrode area, 4 cm^2; scan rate, 10 mV/s; for pH 4.72, acetate buffer was used, whereas for pH 9.32, borate buffer was used.

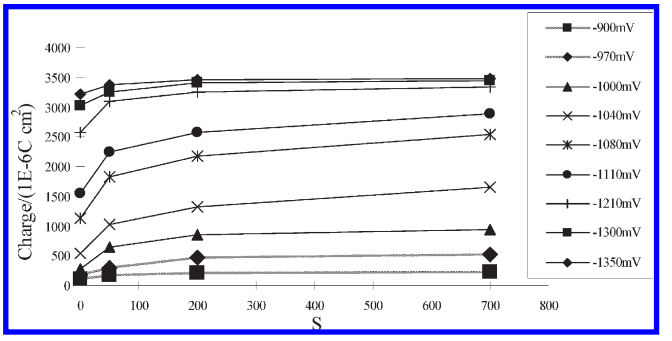

Figure 11. Charge on oxidation peaks in 0.5 M Na_2SO_4 + 50 mM $Na_2B_2O_4$ + 1 mM GeO_2 pH 9.32 solution as a function of holding time at different potentials.

oxidation of the deposited Ge species as a function of solution pH obtained by holding the potential in the hydrogen evolution range for 600 s: −600 mV for pH 1.21, −1150 mV for pH 4.72, −1500 mV for pH 9.32, and −1600 mV for both pH 12.36 and 12.93. pH 9.32 resulted in the maximum coverage.

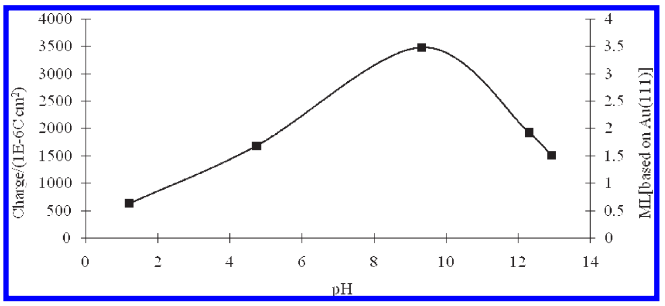

Figure 12. Maximum germanium deposition in 1 mM GeO_2 + 0.5 M Na_2SO_4 solutions as a function of pH. For pH 4.72, acetate buffer was used, whereas for pH 9.32, borate buffer was used.

We assume that Ge within the Au−Ge alloy exists in essentially the zero oxidation state whereas Ge on the surface would be present as the hydride or possibly the hydroxide at more positive potentials. Assuming that the deposits were made at potentials sufficiently negative to produce the hydride, the coverages were calculated on the basis of a five-electron process for the top layer of Ge species (GeH to GeO_2) whereas the bottom layers were assumed to be a four-electron process (Au−Ge to GeO_2 + Au).

The question is then, why does the coverage of Ge species exhibit this behavior as a function of pH? It appears that the Moiré structure is formed regardless of pH but at pH-dependent rates. However, the amounts deposited are a function of pH, and the reasons for this are not clear. Ehlers et al. have proposed a mechanism that may account for the observation. It involves the formation of germanium radicals[50] whose existence has also been suggested in the hydrogen evolution on Ge surface.[53,56,57] At present, kinetic data to prove or disprove such a mechanism was not obtained by this group. There are evidently significant differences between depositions in an aqueous versus a nonaqueous or ionic liquid,[16−18] where the amounts deposited are not limited.

(56) Memming, R.; Neumann, G. *J. Electroanal. Chem.* **1969**, *21*, 295.
(57) Ehlers, C.; Konig, U.; Schultze, J. W. *Electrochim. Acta* **2003**, *49*, 129–135.

Conclusions

This article describes the electrodeposition of germanium on gold substrates from aqueous solutions. The deposition appeared to start with the reduction of a Ge(IV) species to form $GeOH_{(ad)}$, with subsequent reduction to $GeH_{(ad)}$. Using in-situ STM, during deposition at the more positive potentials, two low-coverage structures were observed. The well-ordered structures displayed $(\sqrt{3} \times \sqrt{3})R30°$ and (3×3) unit cells and coverages of $^1/_3$ ML and $^4/_9$ ML. Those structures were composed of adsorbed hydroxide species, probably $GeOH_{(ad)}$. At more negative potentials, the hydroxide species converted to hydride and the coverage increased, resulting in the formation of a structure at 0.8 ML displaying very smooth, large domains of a structure characterized by a Moiré pattern. In most cases, the use of more negative potentials for longer times resulted in the formation of a disordered Au−Ge alloy on the surface. The alloy formation was reversible in a limited potential region, but at more negative potentials, the surface became irreversibly disordered.

The amounts of Ge deposited varied with pH, though each pH appeared to result in a surface-limited amount of Ge. The maximum amount was formed using a pH 9.32 solution, where 3.5 ML were formed. Though the pH appeared to have a strong influence on how much Ge was deposited, the concentration of the Ge(IV) precursor did not. Deposits were formed more quickly from higher-concentration Ge(IV) solutions, but the net amounts deposited did not change.

Acknowledgment. Support for this project was provided by the National Science Foundation, Division of Materials Research.